Strongly interacting matter at RHIC: experimental highlights

Vitaly A. Okorokov

National Research Nuclear University - MEPhI
(Moscow Engineering Physics Institute)

Outline

1. Introduction

2. Selected recent results
   - sQGP properties
   - Discrete symmetries
   - Phase I of the BES

3. Near future plans

4. Summary

Key tasks for HIC program

Study of properties of strongly interacting matter under extreme conditions is very important for several domains: QCD, cosmology and relativistic astrophysics, i.e. has interfield importance.

1. Key questions under discussion:

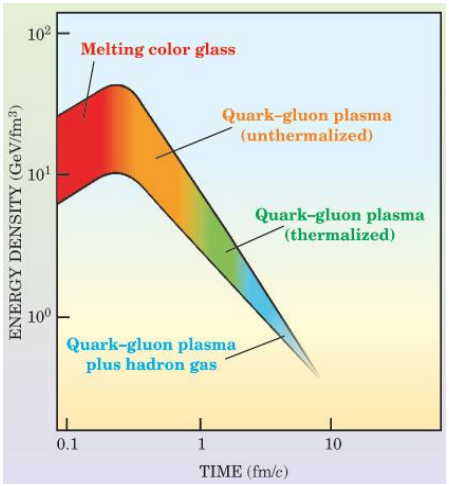

- properties of sQGP,

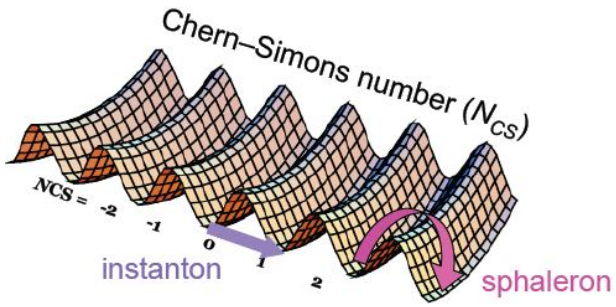

- novel properties of QCD symmetries,

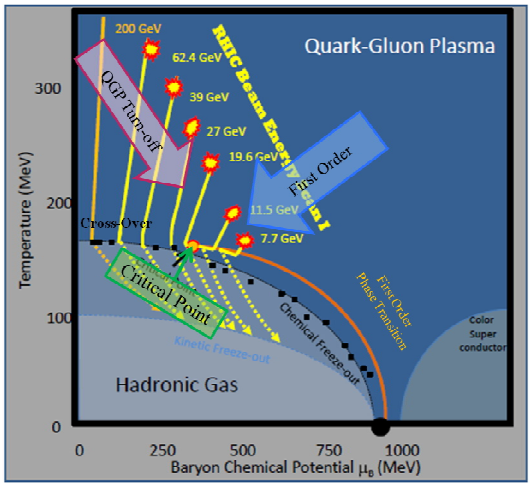

- features of QCD phase diagram (location of CP, etc.).

2. Key problems outside the talk:

- exotic particles and antimatter, effects of cold nuclear matter, spin physics.

BROOKHAVEN NATIONAL LABORATORY

RHIC facility

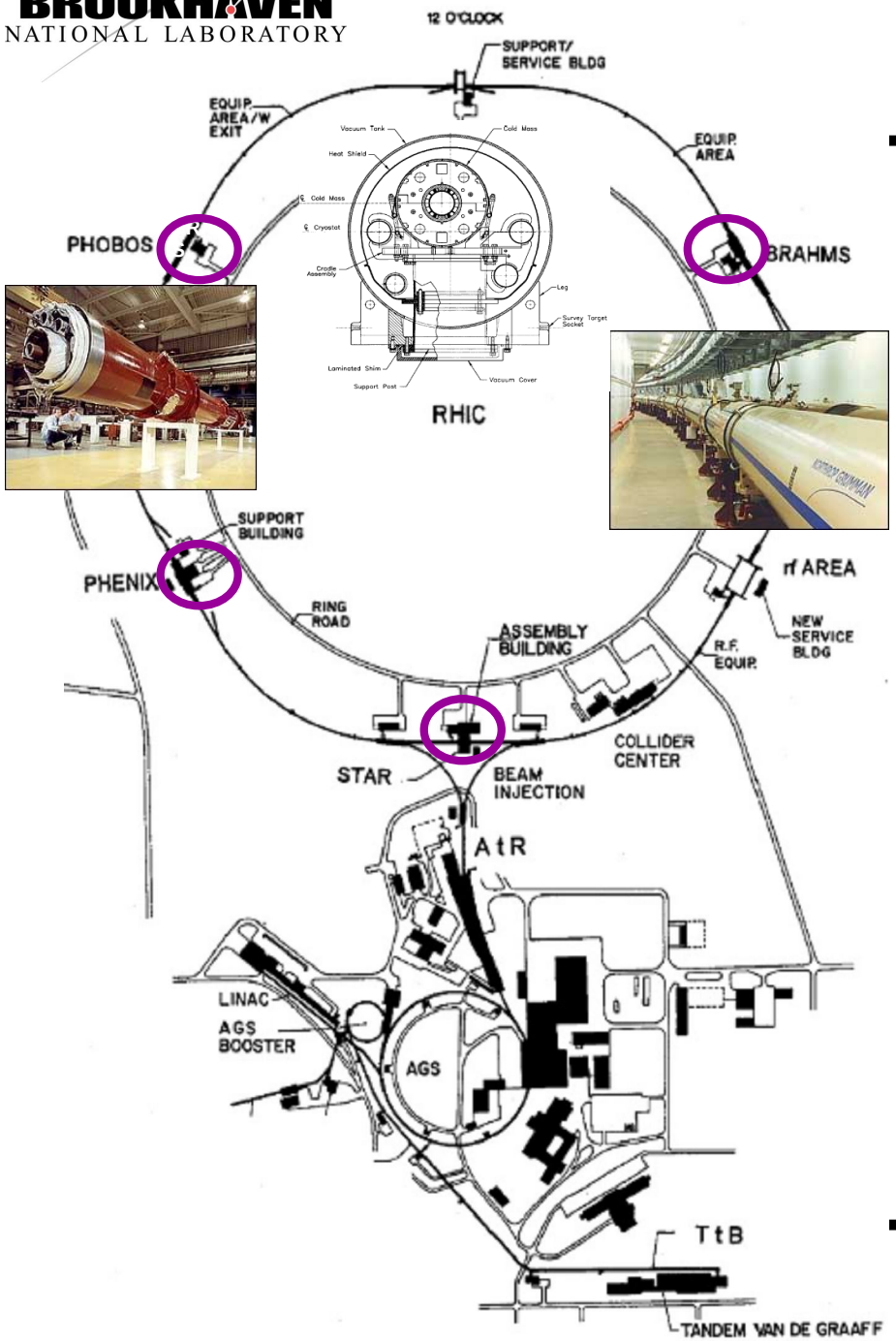

Relativistic Heavy Ion Collider

1. The complex was designed and was built for investigations in QCD field specially.

2. Experiments
- large: PHENIX and STAR continue to collect new data;

- small: BRAHMS and PHOBOS were finished some years ago.

3. **14** successful physics Runs since 2000 year:

- ion collisions
  Cu+Cu, Au+Au, U+U;
  d+Au, He^3+Au, Cu+Au
at $\sqrt{s_{NN}}$ = 7.7, 9.2, 11.5, 14.5, 19.6, 22.4, 27.0, 39.0, 62.4, 130, 193 and 200 GeV (mostly for Au beams);

- p+p collisions at $\sqrt{s}$ = 62.4, 200, 410, 500 and 510 GeV with longitudinal and transverse polarized beams also.

RHIC. NPA 499, 235 (2003).

Event shape: observables

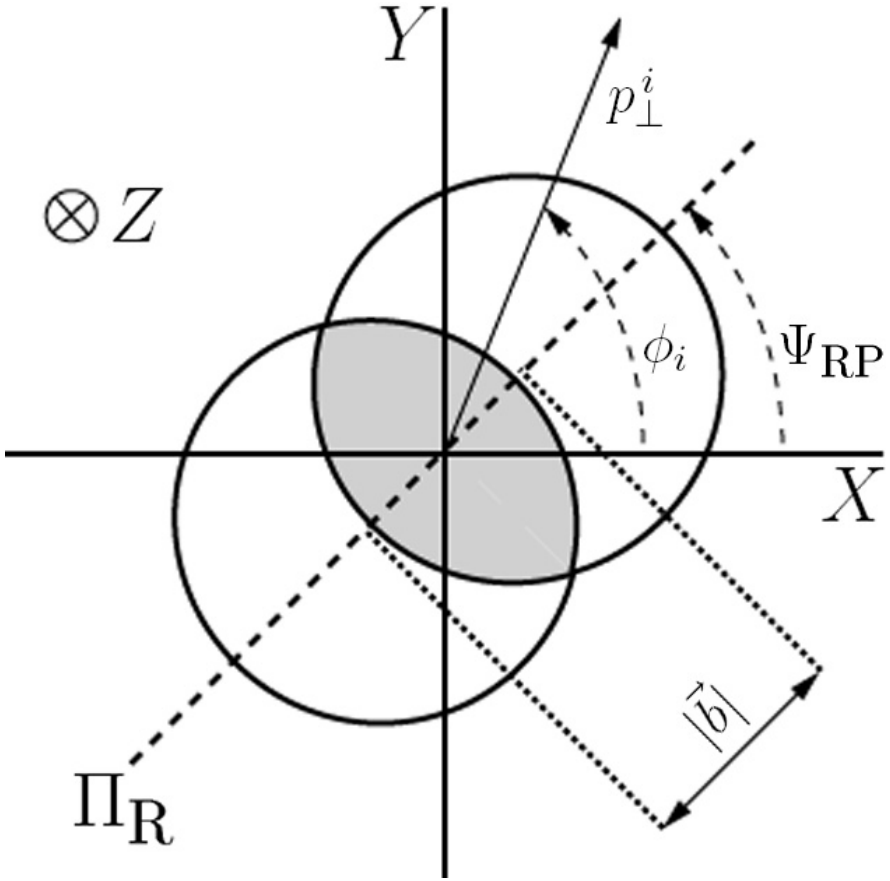

Scheme for non-central ion collisions.

Definition:
the reaction plane – plane contains the beam axis and vector of impact parameter.

Fourier expansion of the triple differential invariant distribution for particles of some *i* type:

Voloshin S.A., Zhang Y. ZPC 70, 665 (1996); Voloshin S.A. PRC 70, 057901 (2004).

$$E\frac{d^3N_i}{d\vec{p}} \propto 1+2\sum_{n=1}^{\infty}\sum_{j=1}^{2} k_{j,n}^{i} F_j[n\Delta\phi_{\mathrm{RP}}^{i}],$$

$$F_{1[2]}(x) \equiv \cos[\sin](x),$$

$$\Delta\phi_{\mathrm{RP}}^{i} = \phi_i - \Psi_{\mathrm{RP}},\ \phi_i = \tan^{-1}(p_y^i / p_x^i),$$

$$k_{1,n}^{i} \equiv v_n^i = \left\langle \cos[n\Delta\phi_{\mathrm{RP}}^{i}] \right\rangle,$$

$$k_{2,n}^{i} \equiv a_n^i = \left\langle \sin[n\Delta\phi_{\mathrm{RP}}^{i}] \right\rangle.$$

- v_n – collective flow – indicates the strength of P-even collectivity,
- a_n characterizes the strength of P-odd correlations.

v_n for neutral mesons

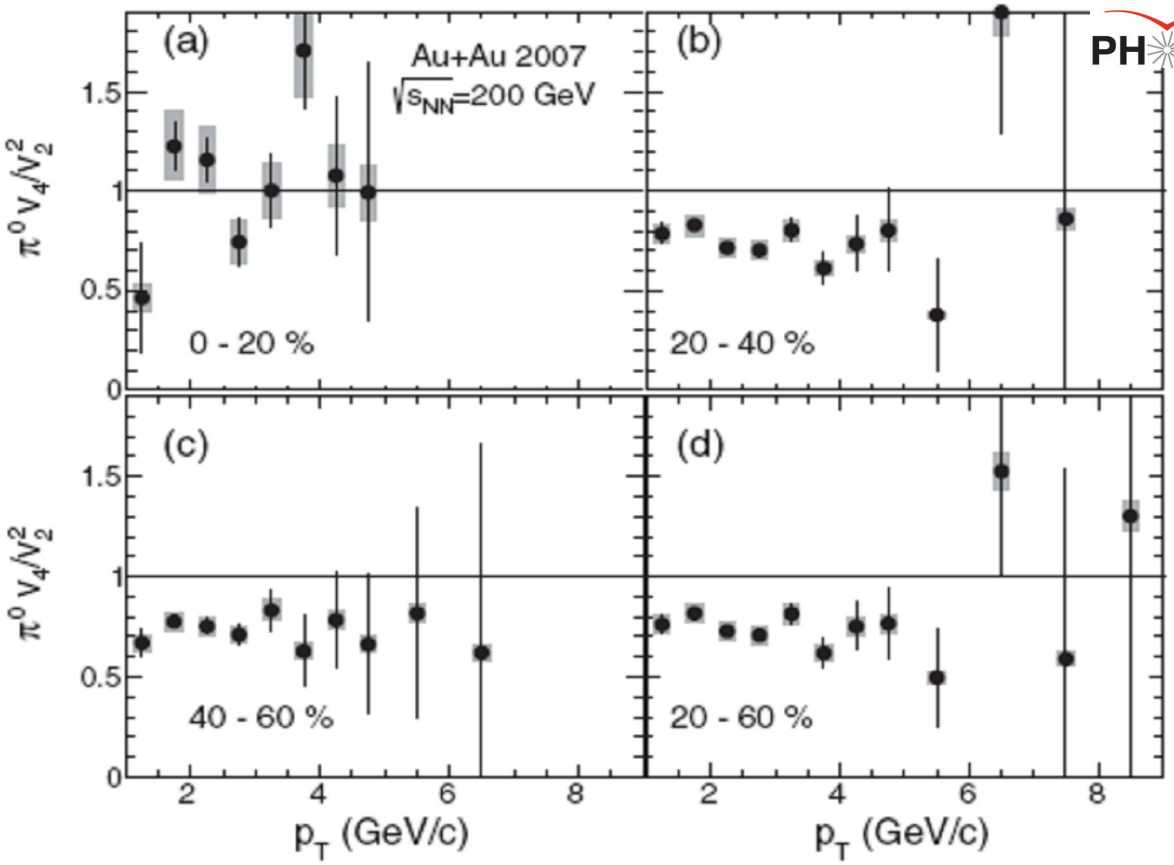

The ratio v_4 / v_2^2 vs transverse momentum for π^0 mesons. The shade boxes represent the systematic uncertainties. PRC 88, 064910 (2013).

- The ratios of v_n coefficients shown above are independent on p_T with a magnitude in the range ~ 0.8 – 1.0 depending on the centrality bin which may reflect the combined effects of fluctuations in the initial collision geometry and finite viscosity in the evolving medium.

v_n in viscous environment

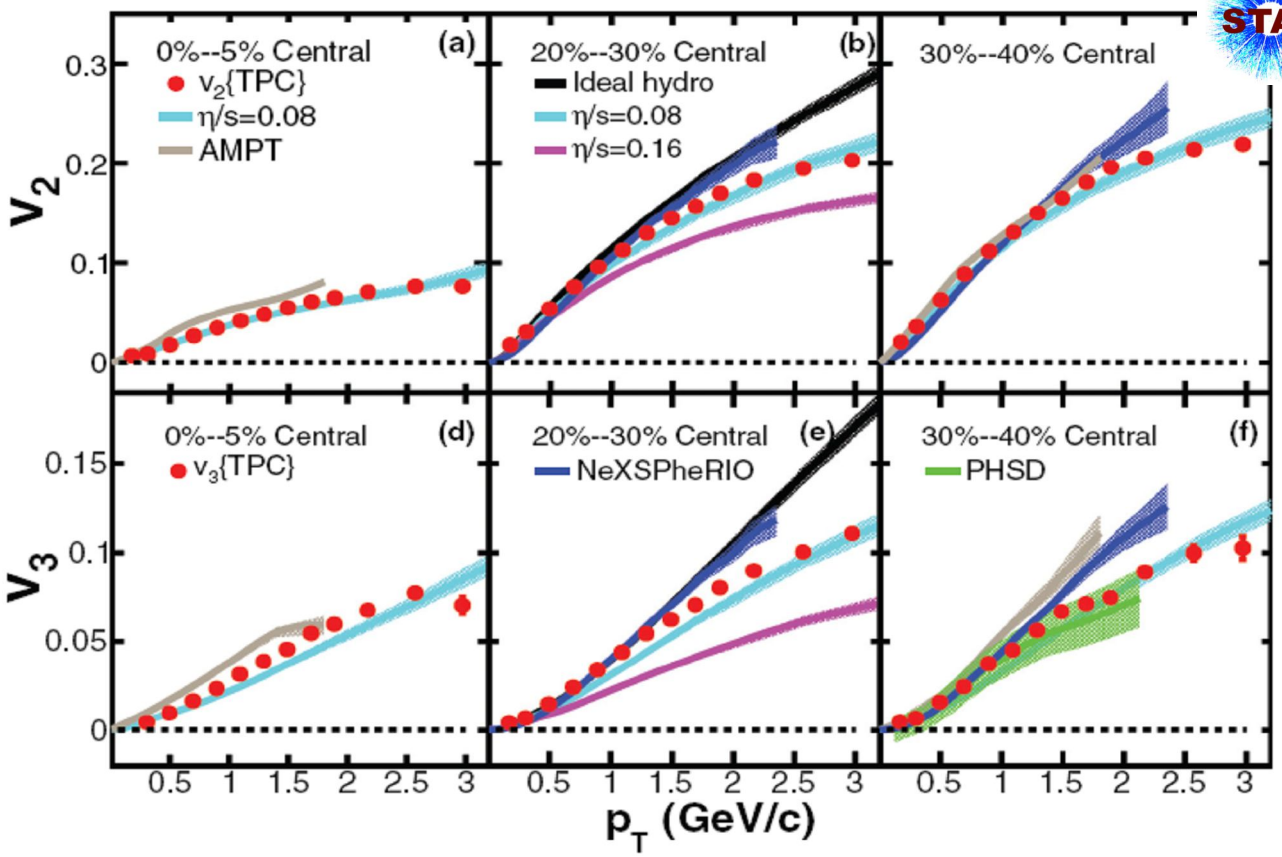

p_T–Dependence of v_2 and v_3 for charged particles in Au+Au collisions at $\sqrt{s_{NN}}$ = 200 GeV in comparison with model calculations. Initial conditions come from MC Glauber model for all hydrodynamic calculations. PRC 88, 014904 (2013).

- The agreement between experimental data and viscous hydro calculations for η/s = 0.08 is good.

- This estimation is in the range η/s = 0.06 – 0.21 extracted from study of correlation function on transverse momentum.
PLB 704, 467 (2011); PRC 87, 064902 (2013).

Path-length sensitive measurements

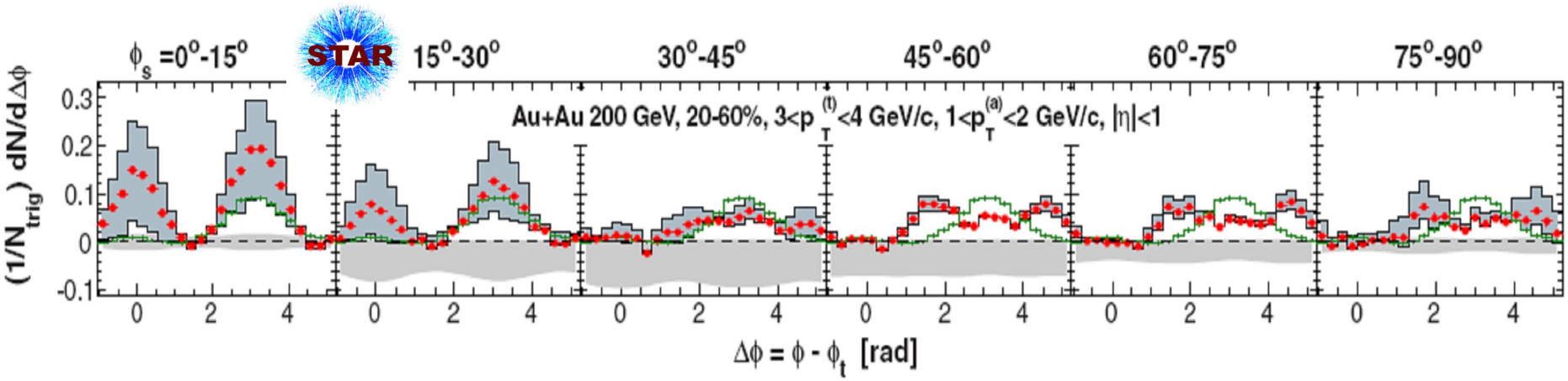

Dihadron azimuthal correlations in various ranges of $\phi_s = |\phi_t - \Psi_{RP}|$ with background subtracted. For comparison, the inclusive dihadron correlations from d+Au are presented as the green histograms.
PRC 89, 041901 (2014).

- The away side peak shows a modification from d+Au data, varying with ϕ_s. This observation agrees with increasing of strength of jet quenching with growth of the jet path inside hot matter.

- This more detailed study confirms the first measurement of path-length dependence of jet quenching.
PRL 93, 252301 (2004).

- There is finite near-side long-range pseudorapidity correlation (ridge) in the in-plane direction ($\phi_s \sim 0$).

Ridge in d+Au collisions

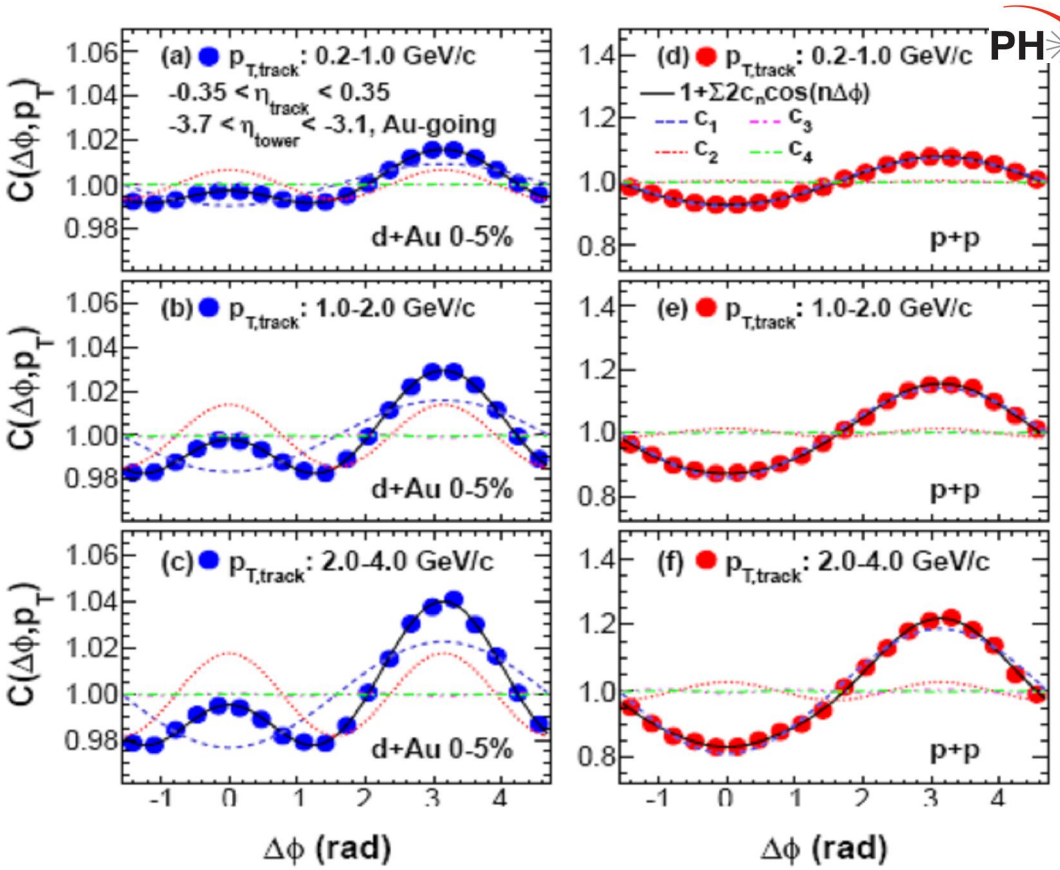

The azimuthal correlation functions for different track p_T selection in d+Au and +p collisions at $\sqrt{s_{NN}}$ = 200 GeV.
arXiv: 1404.7461 [nucl-ex].

- The ridge is observed in d+Au at RHIC as well as in p+Pb at LHC.

- The ridge may be formed by soft particles. Moreover, possibly, there is the same mechanism for ridge creation in both d+Au and p+Pb collisions.
PRL 105, 022301 (2010); 111, 212301 (2013).

J/ψ suppression in A+A collisions

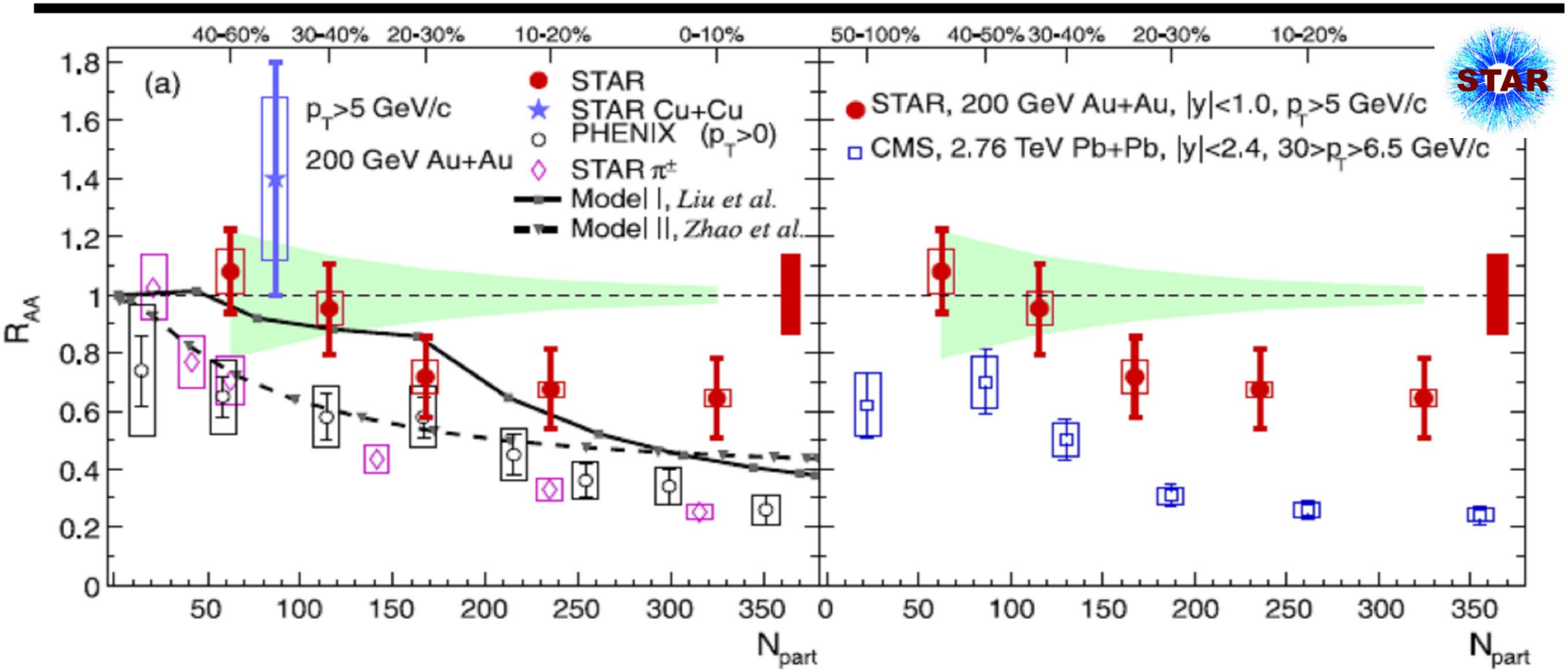

R_{AA} vs centrality for high-p_T J/ψ in comparison with (a) some measurements at RHIC and models; (b) high-p_T J/ψ from CMS.
PLB 722, 55 (2013).

- The significant suppression is seen for high-p_T J/ψ in central Au+Au collisions. This observation indicates strong interactions of heavy quarks with sQGP.

- Values of R_{AA} for high-p_T J/ψ indicate that the formation time of J/ψ does not significantly change but the energy densities change for LHC energy in comparison with top RHIC energy.

Bottomonium in A+A collisions

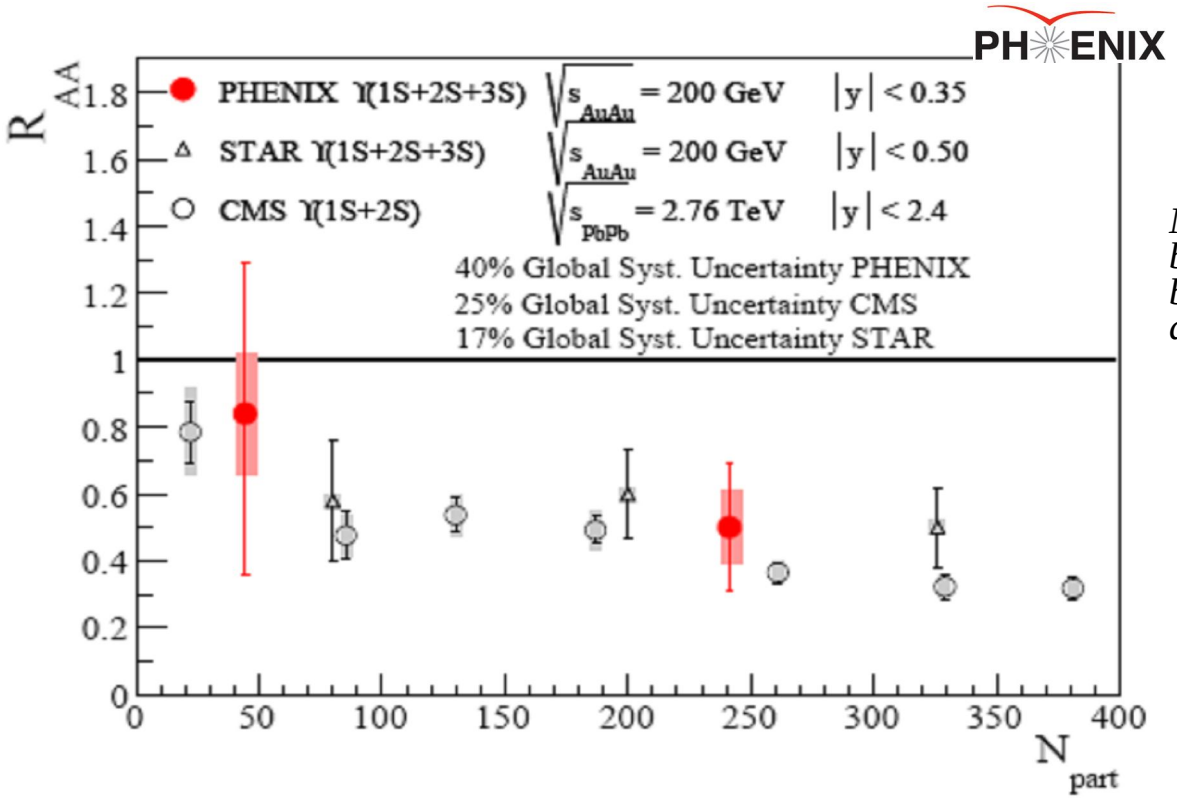

Nuclear modification factor for centrality binned data plotted as a function of number of participants in various experiments. arXiv: 1404.2246 [nucl-ex].

- The values of nuclear modification factor for bottomonium agree with different experiments.
- R_{AA} is consistent with the complete suppression of the bottomonium excited states (Υ(2S+3S) and χ_B).
- R_{AA} is in qualitative agreement with most calculations assuming no cold nuclear matter effects.

Chiral effects in sQGP

- The interplay between extremely strong magnetic field (B) and sQGP created in the HIC makes possible some important effects, in particular, the CME and CSE.
Kharzeev D.E., Annals of Phys. 325, 205 (2010).

- The chiral magnetic effect (CME) is the phenomenon of electric charge separation along the axis of applied magnetic field in the presence of fluctuating topological charge.

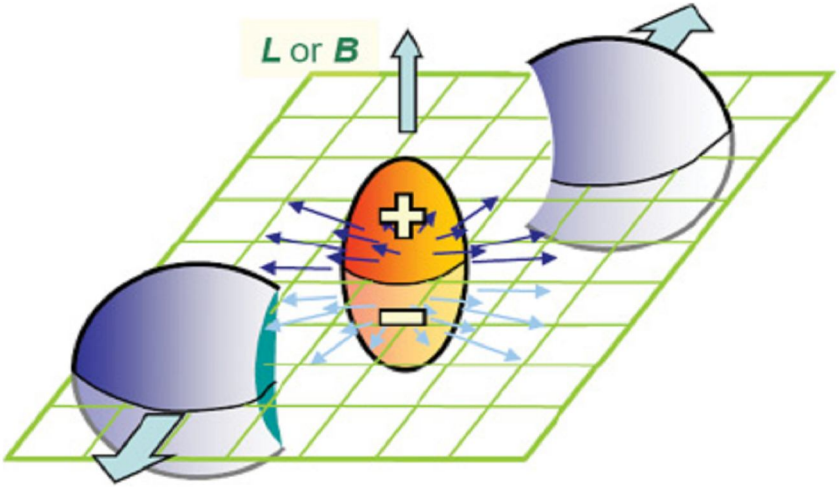

*Schematic view of the charge separation along the system orbital momentum **L** (magnetic field **B**). The orientation of the charge separation fluctuates in accord with the sign of topological charge.*
PRL 103, 251601 (2009); PRC 81, 054908 (2010).

- The chiral separation effect (CSE) refers to the separation of chiral charge along the axis of external magnetic field at finite density of vector charge (e.g. at finite baryon number density).

- The resulting vector / axial current at number of colors N_c and finite axial / vector potential $\mu_{A/V}$ is given by

$$\mathbf{j}_{V/A} = (N_c e/2\pi^2)\mathbf{B}\mu_{A/V}.$$

Experimental signal for CME

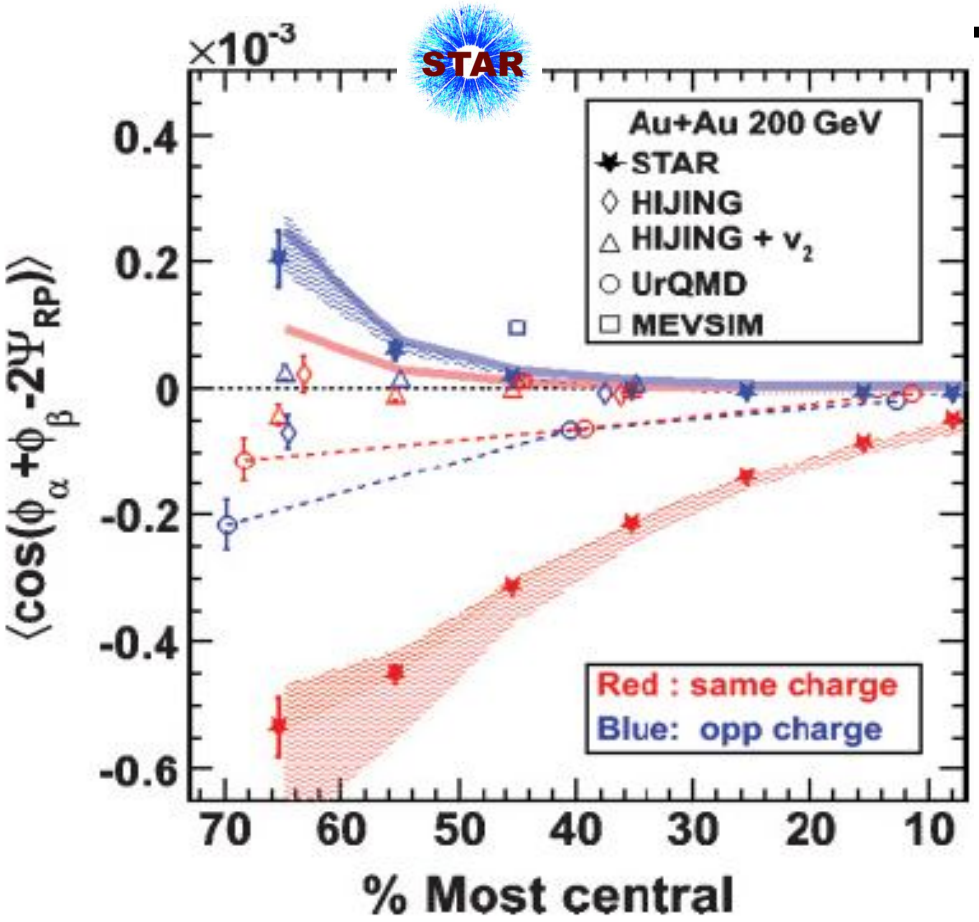

$$\gamma_{\alpha\beta} \equiv \langle \cos(\phi_\alpha + \phi_\beta - 2\Psi_{RP}) \rangle = \langle \cos(\phi_\alpha + \phi_\beta - 2\phi_c) \rangle / v_{2,c}.$$

Centrality dependence of $\gamma_{\alpha\beta}$ in comparison with some model calculations.
PRL 103, 251601 (2009); PRC 81, 054908 (2010).

- Charge separation has been observed in experiments. Qualitatively, the results mostly agree with the magnitude and gross features of the theoretical predictions for local parity violation in HIC.

- There is no model without CME which can describes all experimental results simultaneously, especially the centrality dependence of same-sign correlator.

Tests for CME: preliminary results

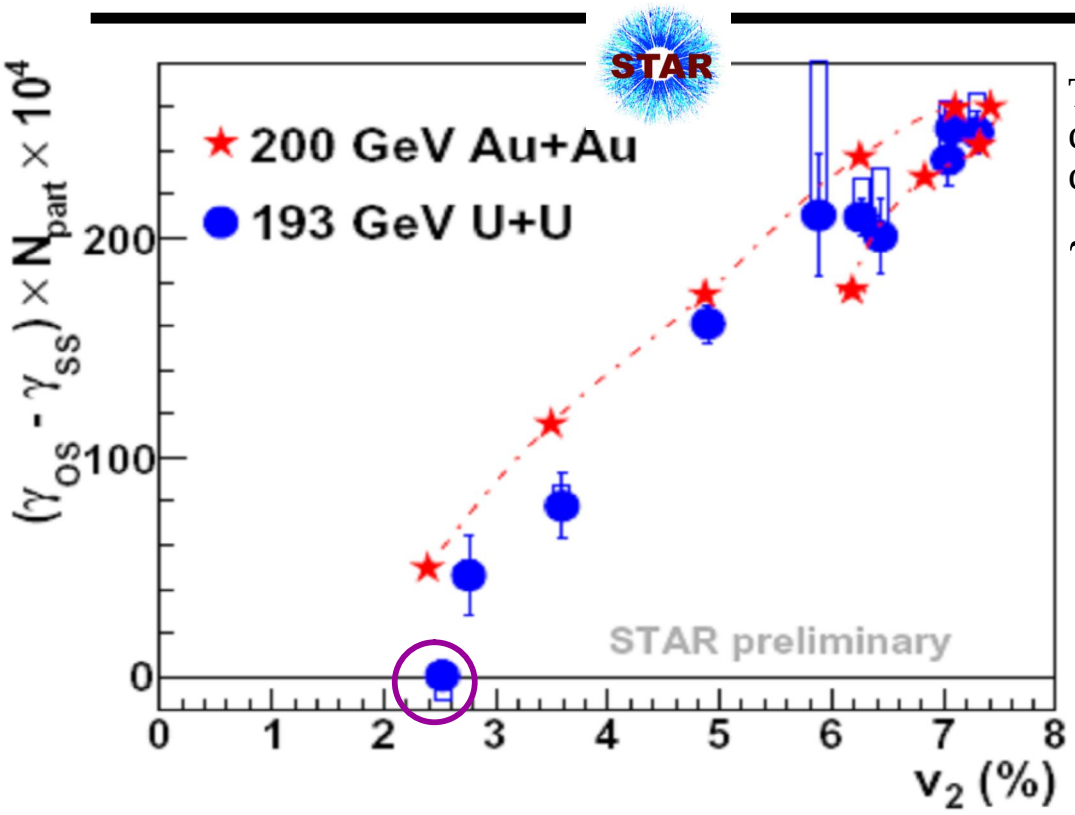

The charge separation could be due to charge conservation / cluster $v_{2,cl}$. In this case:

$$\gamma_{\alpha\beta} \propto \langle \cos(\phi_\alpha + \phi_\beta - \phi_{cl}) \rangle_{cl} v_{2,cl}.$$

The CME-sensitive observable vs v_2.
G. Wang. NPA 904-905, 248c (2013).

- In both Au+Au and U+U, the signal roughly increases with v_2, seemingly following the background trend described by relation above.

- **But** in 0-1% very central U+U collisions the signal disappears as expected by the CME, while v_2 is still ~ 2.5%. One can (preliminary) conclude: there is a finite contribution from CME.

Partonic vs hadronic d.o.f.: charge separation

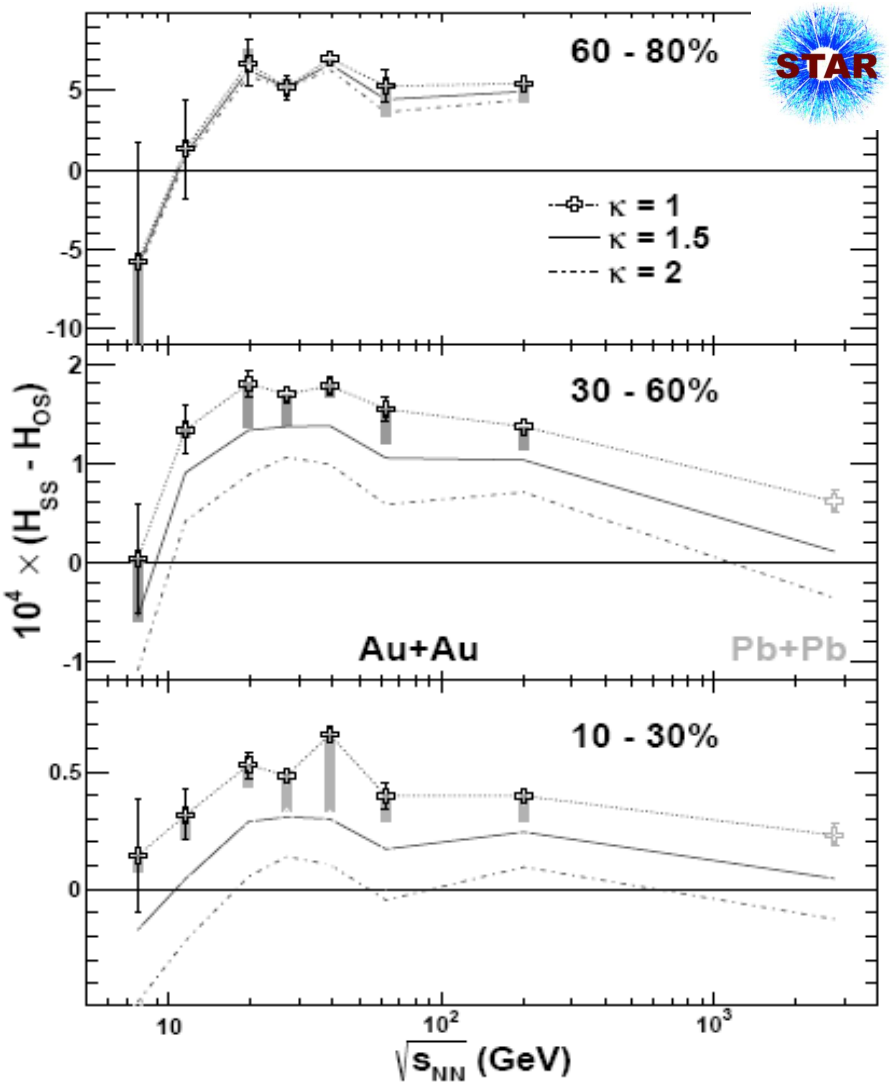

$$H^{\kappa} = (\kappa v_2 \delta - \gamma) / (1 + \kappa v_2),$$
$$\gamma \equiv \langle \cos(\phi_\alpha + \phi_\beta - 2\Psi_{RP}) \rangle,$$
$$\delta \equiv \langle \cos(\phi_\alpha - \phi_\beta) \rangle.$$

Correlator difference as a function of $\sqrt{s_{NN}}$. The default values (dotted curves) are for $H_{\kappa=1}$, and the solid (dash-dot) curves are obtained with κ = 1.5 (κ = 2). arXiv: 1404.1433 [nucl-ex].

- The background contributions are reduced for new observables $H_{\alpha\beta}$ (α, β = +, -).
- Charge separation, studied via correlator difference, decreases steeply at $\sqrt{s_{NN}} < 19.6$ GeV.
- The trend of $(H_{SS} - H_{OS})$ may be consistent with local parity violation because there should be a smaller probability for the CME at lower energies where the hadronic phase plays a more dominant role than the quark-gluon phase.

R_{AA} for J/ψ vs $\sqrt{s_{NN}}$

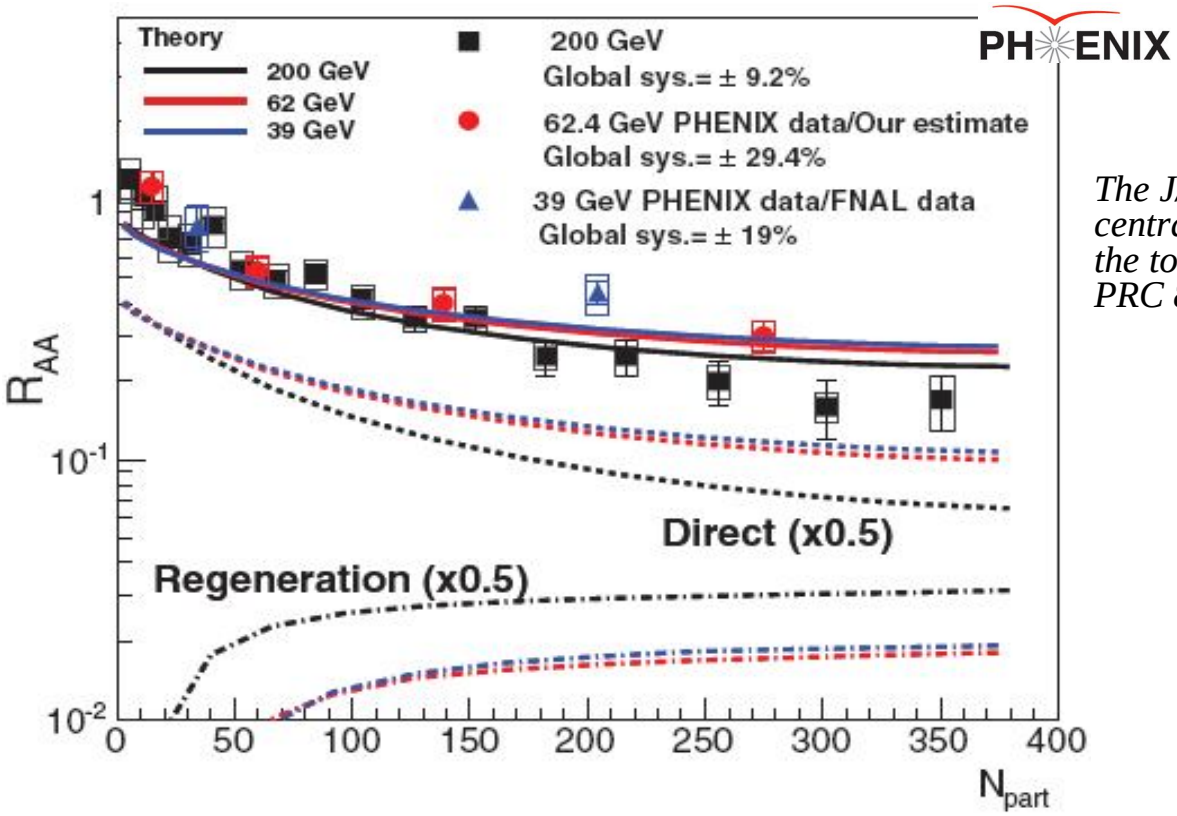

The J/ψ nuclear modification factor R_{AA} vs centrality. Calculation results are shown for the total R_{AA} and the separate contributions. PRC 86, 064901 (2012).

- Similar suppression is observed in the energy domain $\sqrt{s_{NN}}$ = 39 – 200 GeV with slightly less suppression at $\sqrt{s_{NN}}$ = 39 GeV in most central events.

- Experimental R_{AA} values are consistent with theoretical calculations dominated by the balancing effects of more sQGP suppression as well as more J/ψ regeneration for higher energy collisions.

1-st order PT: v_1 slope

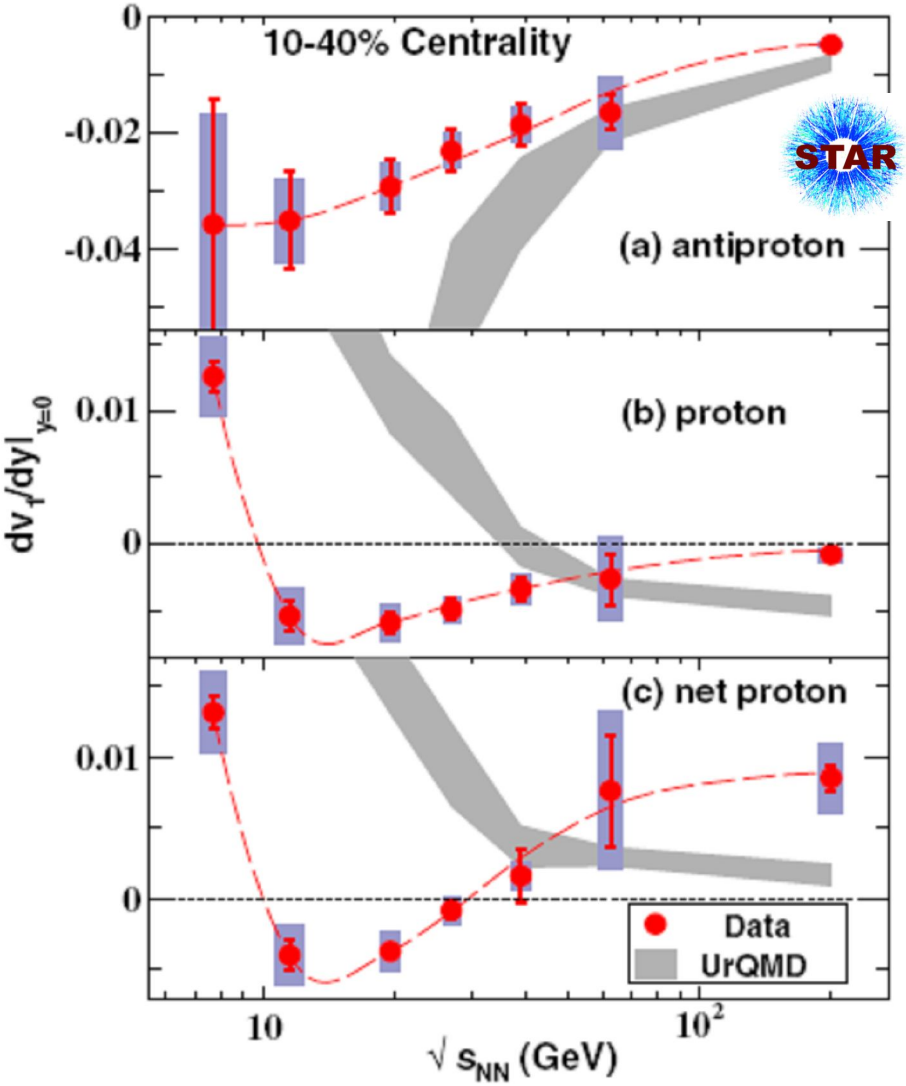

Cubic fit of experimental v_1-distribution:

$$v_1(y) = av_1 + bv_1^3,\ dv_1/dy \equiv a.$$

Directed flow slope (dv_1 / dy) near midrapidity vs $\sqrt{s_{NN}}$ for Au+Au. Dashed curves are a smooth fit to guide the eye.
PRL 112, 162301 (2014).

- The observed minimum for protons and net-protons resembles the hydrodynamically predicted softest point collapse of flow and is possible signature of a 1-st order phase transition between hadronic matter and deconfined phase.

BES phase-II: luminosity improvements

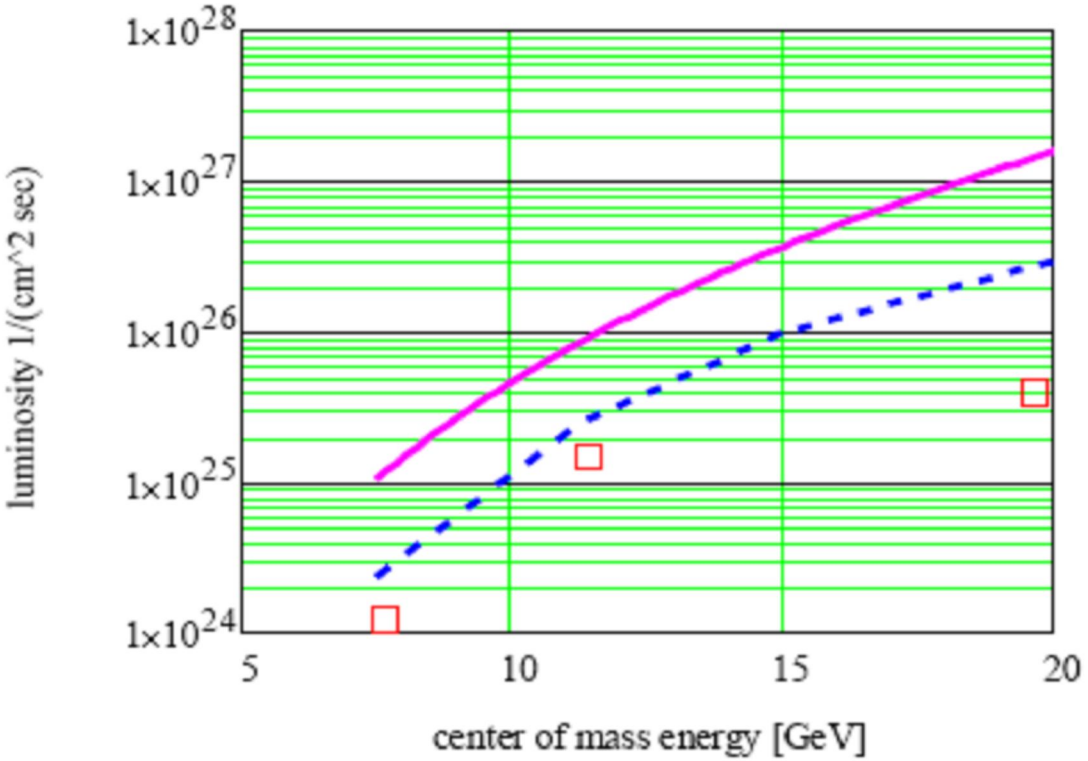

Average luminosity in RHIC with Au beam and electron cooling. Red squares: measured average store luminosity in BES-I. Blue / magenta line: minimum / maximum improvement with cooling.

- Every energy for $\sqrt{s_{NN}} \approx 7 – 20$ GeV are available with electron cooling.
- Electron cooling together with longer beam bunches for phase-II increases luminosity by a factor of 4 – 15 compared to phase-I.

BES phase-II: projections

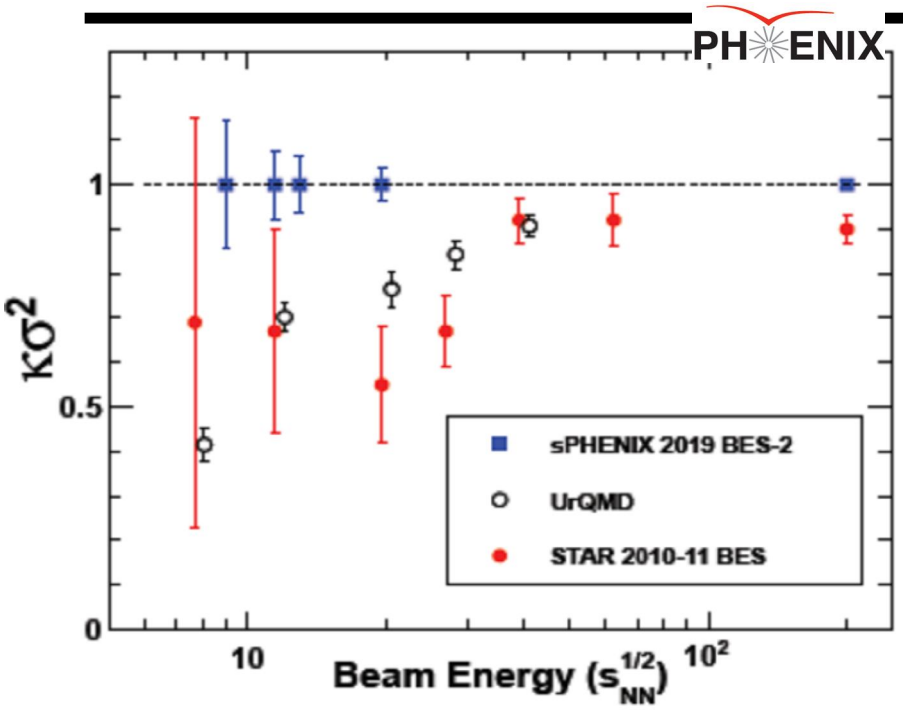

Estimates for sPHENIX sensitivity to measurement of net-proton $\kappa\sigma^2$ for Au+Au collisions vs $\sqrt{s_{NN}}$. BES II. PHENIX White Paper v. 1.0.

- PHENIX and STAR will have much smaller error bars for $\sqrt{s_{NN}} < 19.6$ GeV for BES phase-II.
- Crucially important for precise exploration of QCD phase diagram and for cross check of results of the BES phase-I.

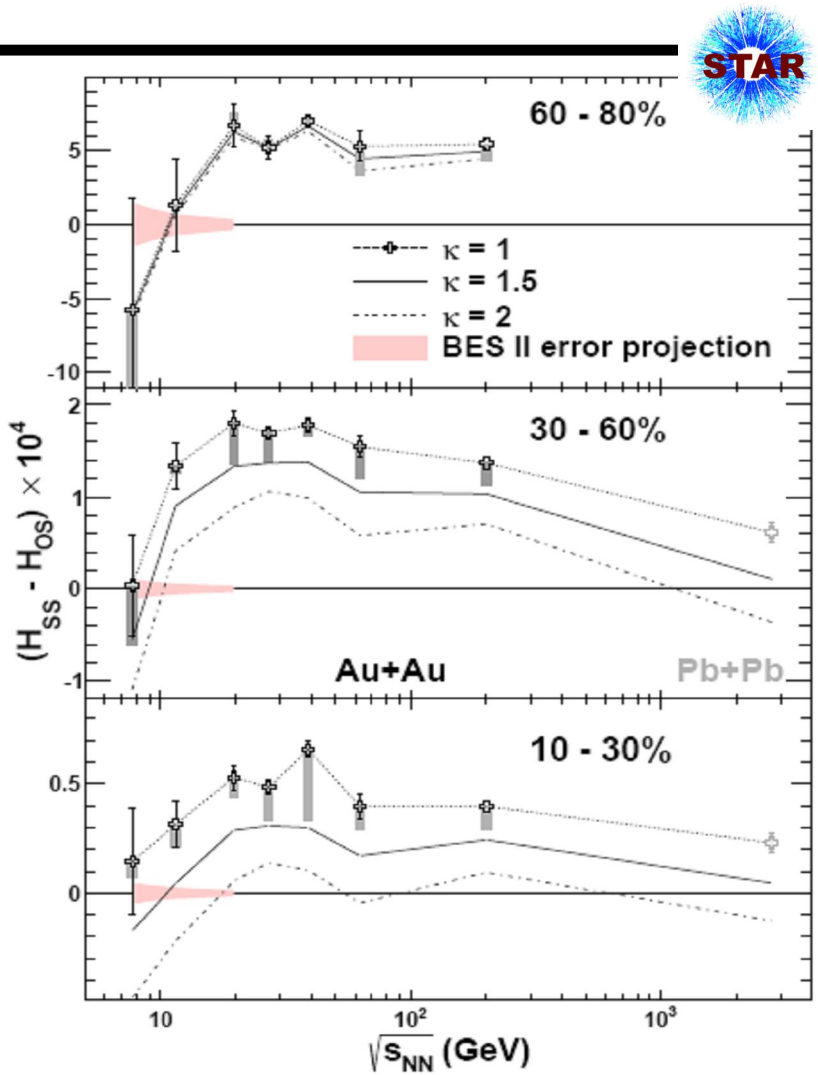

Observable for study of CME vs $\sqrt{s_{NN}}$ is shown with error projections for BES phase-II. BES II. STAR White Paper v. 6.9.

PHENIX upgrades

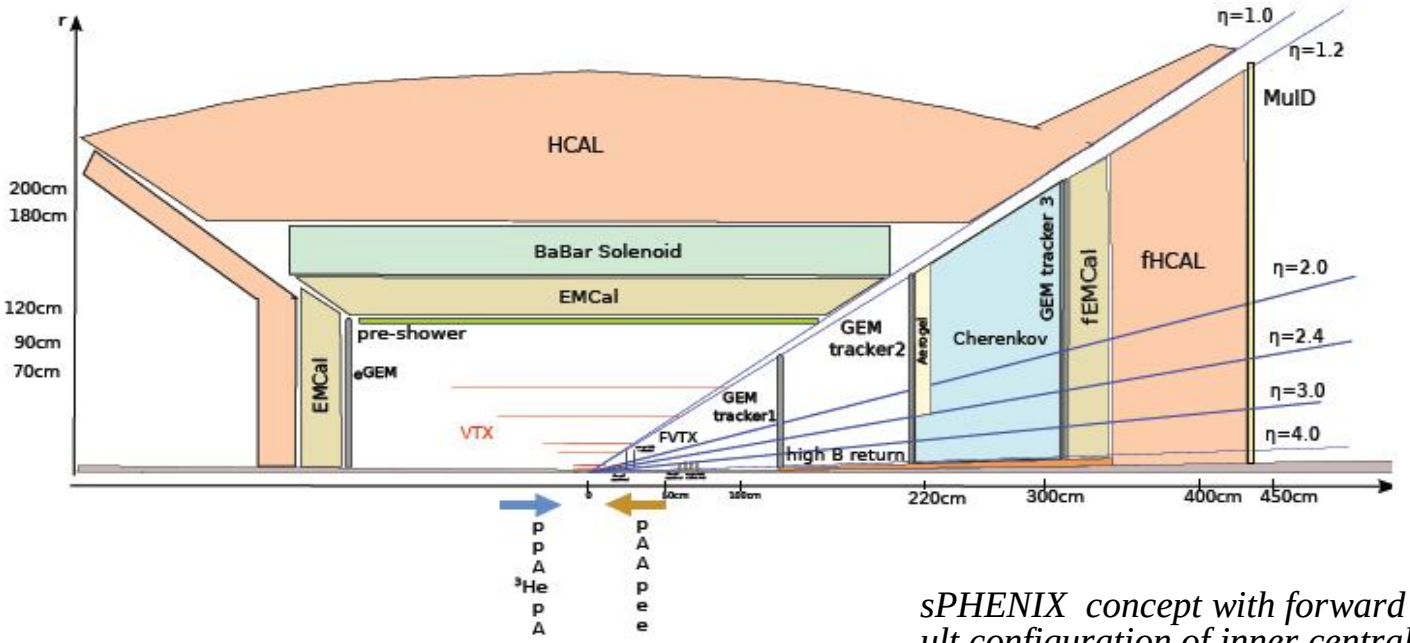

sPHENIX concept with forward detector and default configuration of inner central part.
arXix: 1207.6378 [nucl-ex]; 1402.1209 [nucl-ex].

- The future PHENIX plans are built around extensive upgrade – sPHENIX. This upgrade consists of new large acceptance EM and hadronic calorimetry built around the superconducting solenoid from BaBar experiment at SLAC. There are three options of inner part, in particular, with TPC.

- sPHENIX will make key new measurements of hard probes of sQGP as well as studies in the framework of phase-II of BES in 2019.

STAR upgrades for phase-II

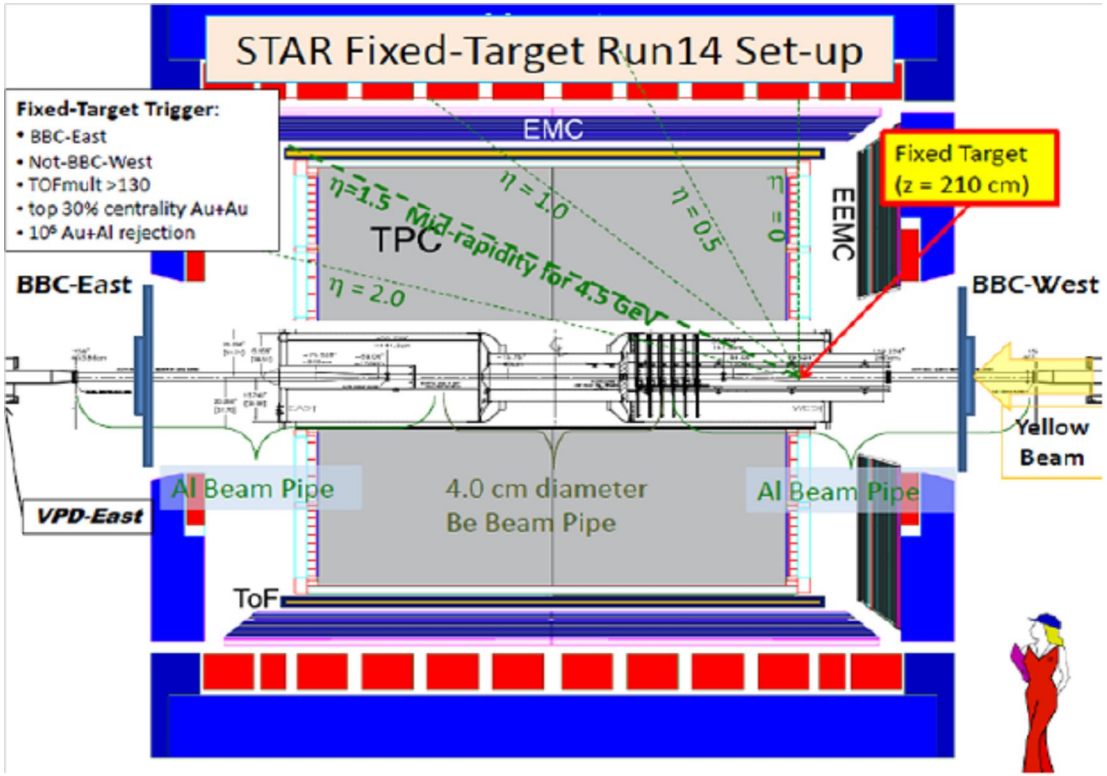

A schematic diagram of STAR showing the fixed-target location for the test in 2014. Target – 1 mm thick gold foil. BES II. STAR White Paper v. 6.9.

- New event plane detector – EPD which will be independent from main detector and very inportant for flow and fluctuation analyses.

- Upgrade of inner sectors of TPC – iTPC will increases of TPC acceptance to $\eta \sim 1.7$, improves resolutions and efficiencies.

- Fixed target part of phase-II: down to $\sqrt{s_{NN}} \approx 4$ GeV and reach to region of compressed baryonic matter.

Summary

1. Present

- important influence of collision geometry on final-state shape, estimations of η/s close to the quantum limit $1/4\pi$;
- path-dependent energy loss and significant suppression of heavy quarks;
- «ridge» – general feature of event structure in various collision and in wide energy range (RHIC – LHC);
- experimental indications on topology induced local parity violation in strong interactions;
- experimental signals for dominance of partonic degrees of freedom at $\sqrt{s_{NN}} \geq 39$ GeV and for transition to dominance of hadronic phase on quark-gluon one at $\sqrt{s_{NN}} < 19.6$ GeV.

At RHIC the new field of fundamental investigations is developed – «QCD of condensed matter» which is important both for physics of strong interactions and cosmology, relativistic astrophysics.

2. Future

- detailed plans for physics studies and detector upgrades
- until ~ 2022 (RHIC core program): precise study of sQGP and phase-II of the BES;
- after ~ 2022 (eRHIC): 3D-structure of nucleon and nuclei, dense gluon matter.

Thank you for attention